

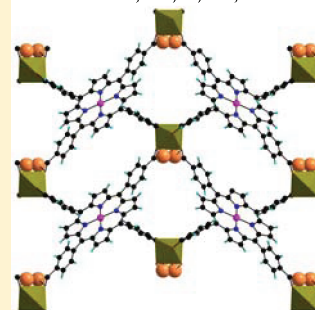
Series of Porous 3-D Coordination Polymers Based on Iron(III) and Porphyrin Derivatives

Alexandra Fateeva,[†] Sabine Devautour-Vinot,[‡] Nicolas Heymans,[§] Thomas Devic,^{*,†} Jean-Marc Grenèche,^{||} Stefan Wuttke,^{†,⊥} Stuart Miller,[†] Ana Lago,[†] Christian Serre,[†] Guy De Weireld,[§] Guillaume Maurin,[‡] Alexandre Vimont,[⊥] and Gérard Férey[†][†]Institut Lavoisier, UMR CNRS 8180, Université de Versailles Saint-Quentin-en-Yvelines, 45 avenue des Etats-Unis, 78035 Versailles cedex, France[‡]Institut Charles Gerhardt Montpellier, UMR CNRS 5253, UM2, ENSCM, Place E. Bataillon, 34095 Montpellier cedex 05 France[§]Laboratoire de Thermodynamique, Faculté Polytechnique, Université de Mons, 20 place du Parc, 7000 Mons, Belgium^{||}Laboratoire de Physique de l'Etat Condensé, UMR CNRS 6087, Université du Maine, 72085 Le Mans Cedex, France[⊥]Laboratoire Catalyse et Spectrochimie, ENSICAEN, Université de Caen, CNRS, 6 Bd Maréchal Juin, 14050 Caen, France

Supporting Information

ABSTRACT: A new series of 3-D coordination polymers based on iron(III) and nickel(II) tetracarboxylate porphyrin (Ni-TCPP) have been produced using solvothermal conditions. MIL-141(A) solids (MIL stands for Material from Institut Lavoisier), formulated $\text{Fe}(\text{Ni-TCPP})\text{A}\bullet(\text{DMF})_x$ ($\text{A} = \text{Li}, \text{Na}, \text{K}, \text{Rb}, \text{Cs}$, DMF = N,N-dimethylformamide, $x \sim 3$), are built up from three anionic interpenetrated PtS-type networks charge-balanced by alkali cations (A) entrapped inside the pores. MIL-141(A) thus includes three types of cations, two of which may act as coordinatively unsaturated metal sites (Ni^{2+} and A^+). These solids all present a permanent porosity with a reasonably high surface area ($S_{\text{BET}} = 510\text{--}860 \text{ m}^2 \text{ g}^{-1}$) as well as some structural flexibility toward adsorption/desorption processes, modulated in both cases by the nature of A. Thermally Stimulated Current (TSC) measurements indicated that alkali cations are rather homogeneously distributed within the pores, while their interaction with the framework is stronger in MIL-141(A) than in the analogous cation-containing Faujasites X and Y zeolites. Finally, high pressure adsorption isotherms of N_2 and O_2 were measured. Whereas alkali ion-containing zeolites adsorb selectively N_2 toward O_2 , the opposite is observed for MIL-141(A). This result is interpreted in light of the TSC data and the possible preferential interaction of the porphyrinic linker with O_2 .

KEYWORDS: coordination polymers, MOFs, porphyrin, cation-containing porous solids, thermally stimulated current, O_2/N_2 separation

MIL-141(A) or $[\text{Fe}(\text{Ni-TCPP})\text{A}]$
 $\text{A}^+ = \text{Li}, \text{Na}, \text{K}, \text{Rb}, \text{Cs}$ 

INTRODUCTION

Porous coordination polymers have attracted a lot of attention over the past decades because of their remarkable abilities in number of applications such as gas storage, separation, catalysis or controlled drug release.¹ More recently, an increasing effort is noticeable in designing more sophisticated organic linkers^{2–25} or metalloligands,^{26–30} in order to develop hybrid materials with novel optic, electronic, or magnetic properties.

In our quest for discovering novel original porous frameworks with multifunctional linkers we particularly focused on porphyrinic building blocks. Actually, metalloporphyrins represent a fascinating class of molecules as they play a key role in nature as oxygen transport in hemoglobin or the photosynthesis in chlorophyll. Because of their photochemical,^{31–37} electrochemical,^{38–45} and catalytic^{46–55} properties they have inspired a huge domain of applications. Many chemists have thus focused their work on the development and study of porphyrins, and a large effort was deployed to develop synthetic methods in porphyrinic chemistry.^{56–58} Indeed, functionalized porphyrins

are now relatively easily accessible and well studied compounds. Especially, their ease of functionalization is of particular interest as it has been clearly demonstrated that tailoring the nature of the substituent or the central metallic ion allows fine-tuning the properties of these metalloligands.^{59–63} It results that the porphyrinic (or phthalocyanines) derivatives appear as attractive building blocks for the preparation of functional hybrid porous solids.^{64–67} Particularly, since the 1990s, many attempts have been reported in order to build up open coordination frameworks based on linkers derived from porphyrins.^{68–72} However, examples of materials stable upon solvent removal and exhibiting a permanent porosity detected by gas sorption are still scarce.^{73–75} More precisely, several solids based on the tetrapropic 5,10,15,20-tetrakis(4-carboxyphenyl)porphyrin (TCPP, see Figure 1a) anionic linker, which can give rise to

Received: August 29, 2011

Revised: September 14, 2011

Published: September 30, 2011

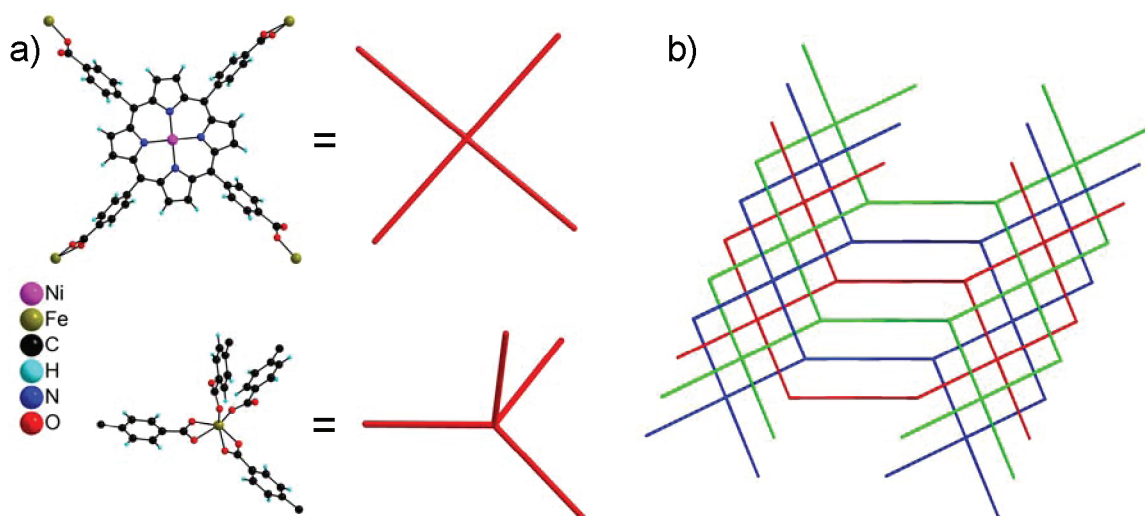


Figure 1. a) The organic (top) and inorganic (bottom) nodes and their schematic representations and b) scheme of the complete structure consisting of three interpenetrated nets with the PtS topology (view along $[1 -4 0]$).

stable neutral frameworks, have been reported. For instance, the groups of Goldberg,^{76–80} Choe,^{81,82} and Kempe^{83,84} published many examples of two- and three-dimensional open frameworks constituted by the TCPP linker and various metallic ions, but no permanent porosity was evidenced in these solids. Another noticeable study was reported by the group of Suslick,⁸⁵ with a 3-D solid based on the Co^{II}-TCPP porphyrinic building block that shows interesting selective adsorption of different liquids, although nitrogen sorption experiments revealed a low BET surface area ($125 \text{ m}^2 \text{ g}^{-1}$). A few years later, Mori et al. published some porous Ru-based solids and their use in catalytic reactions.^{86,87} More recently, Choe et al. reported a Zn-based porous 2-D solid,⁸⁸ and Hupp et al. reported a series of solids based on various metalated TCPP presenting accessible metals sites and a microporosity detected by CO₂ sorption.⁸⁹

Noteworthy, the above-mentioned coordination polymers are mainly based on M^{2+} cations (especially $M^{2+} = \text{Cu, Zn, Cd}$), although it is established that the derived solids are often less stable than those based on more charged cations ($M^{3+} = \text{Al, Cr, Fe, M}^{4+} = \text{Ti, Zr}$), especially regarding to hydrolysis.^{90,91} In this prospect, we have devoted since the past few years much effort on the development of synthetic strategies to prepare such solids.^{92,93} Among them, iron(III)-based solids deserved a special attention, as this cation is one of the most adequate for bio- (very low toxicity)⁹⁴ or redox-related (MOFs as positive electrodes for Li-ion batteries)^{95,96} applications. Nevertheless, only a few Fe^{III}-based MOFs with either *permanent*^{95,97–100} or *dynamic*^{101–103} porosity have been reported so far.

We have thus focused our attention on investigating the reactivity of iron(III) with the nickel–metalated TCPP porphyrin, Ni-TCPP derivative that leads to a novel 3D porous MOF framework, three-times interpenetrated, labeled as MIL-141. This latter possesses an anionic framework counter-balanced by one extra-framework alkali cation A^+ ($A = \text{Li, Na, K, Rb, Cs}$) present within the pores. The first part of this paper deals with the synthesis, structural, thermal, and textural features of the series of MIL-141 solids. In a second step, the characterization of their dielectric relaxation properties by means of Thermally Stimulated Current (TSC) measurements is reported to follow how both the cation distribution within the porosity and the

cation/framework interaction evolve with the nature of the alkali ion embedded in the MIL-141(A). Such information is a crucial point as one would expect that similarly to the case of the cation containing zeolites,^{104–106} the partition of the extra-framework cations influences the distribution of the electron density in the framework and hence the interactions with guest molecules, leading to changes in the adsorption properties of these solids. Preliminary O₂ and N₂ single gas sorption measurements have further been conducted to test the potentiality of these solids for O₂/N₂ separation. Although the specific properties of cation-containing MOFs were already considered for various applications related to gas sorption, such as enhanced H₂ storage^{107–110} or CO₂ capture,^{111–113} in the field of gas separation,¹¹⁴ only a few neutral framework MOFs were considered for O₂/N₂ separation.^{115–122} The so-obtained results are mainly compared to those previously reported for cation containing zeolites that are commonly used as adsorbents in air purification technology.^{123–125}

EXPERIMENTAL SECTION

Synthesis. The porphyrinic linkers were prepared from the corresponding 5,10,15,20-tetrakis(4-methyl benzoate) porphyrins. This later porphyrin was synthesized according to a published procedure,¹²⁶ in a 35% yield and further metalated with NiCl₂ in classical conditions, with 90% yield. The hydrolysis of the ester functions to carboxylic acid was undertaken with the corresponding alkali hydroxide solution (AOH, with $A = \text{Li, Na, K, Rb or Cs}$) in order to control the nature of the alkali cation in the final related MOF structure.

Typical procedure for the synthesis of MIL-141(A) is described below for $A = \text{K}$. 400 mg (0.36 mmol) of the 5,10,15,20-tetrakis(4-carboxyphenyl) nickel porphyrin was reacted with 300 mg (1.1 mmol) of FeCl₃·x(H₂O) and 0.6 mL of 2 M KOH aqueous solution in 50 mL of DMF. The solution was heated at 150 °C in Teflon lined autoclave for 48 h. The solution was then filtered and washed with DMF, water, and acetone. Dark purple single crystals suitable for X-ray diffraction were obtained in mixture with a minor amount of an unidentified red powder. The single-crystals were purified by a density separation technique and obtained as a pure phase in a 55% yield (250 mg).

Characterizations. The Supporting Information contains the details of the different techniques (single crystal and powder X-ray diffraction, thermal analyses (TGA, X-ray thermogravimetry) *in situ*

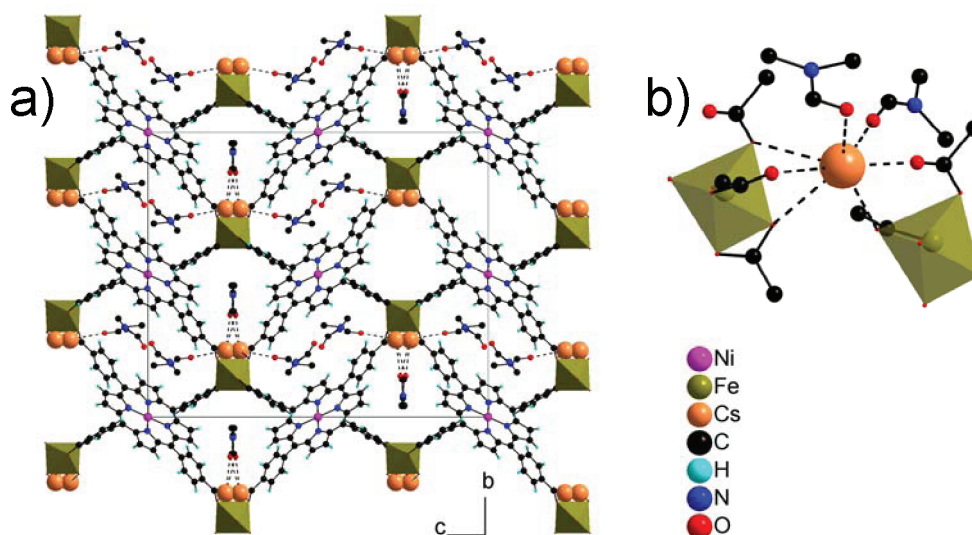


Figure 2. a) View of MIL-141(Cs) along [100]; for the sake of clarity, two channels (top right) are depicted without the DMF molecules. b) Coordination sphere of the Cs⁺ cation; both Cs⁺ and DMF molecules present a positional disorder, only one position is depicted.

infrared and ⁵⁷Fe Mössbauer spectrometries, gas sorption measurements and Thermally Stimulated Current (TSC)) used for the characterization of the solids described in this article. The simulation tools employed for predicting the theoretical accessible surface area for the MIL-141(Cs) solid are also described.

RESULTS AND DISCUSSION

Synthesis. The synthesis of the Fe(Ni-TCPP)A•(DMF)_x (A = Li, Na, K, Rb, Cs; *x* ~ 3) solid or MIL-141(A) has been performed under solvothermal conditions, in DMF and in the presence of an alkali hydroxide aqueous solution. The addition of a base is required in order to deprotonate the carboxylic acid functions and thus facilitate the coordination of the iron ion to the porphyrin. The reaction conditions were optimized in 20 mL reactors and were easily transferred to a larger scale (125 mL reactors) with a good yield (55% after purification). After the crystallization step, regardless the alkali cation used, purple single-crystals suitable for single crystal X-ray diffraction analysis were obtained and purified according to the published density-based procedure.¹²⁷ The EDX analysis (for A = from K to Cs, see Table S4) confirmed the incorporation of the corresponding ion, with a Ni:Fe:A ratio close to 1:1:1. However, a difference of stability between crystals containing light or heavy alkali cations was observed: while the K-, Rb-, and Cs-based solids are stable under ambient atmosphere, MIL-141(Li) and MIL-141(Na) are sensitive to humidity. For this reason, the present article is mainly focused on the properties of the heavier cation containing MIL-141(K, Rb, Cs) solids.

Structural Analysis. Single-crystal and powder X-ray diffraction (see Figure S2) analysis confirmed that all the solids are isostructural and can be obtained in a rather pure crystalline form. MIL-141(A) (A = Li, Na, K, Rb, Cs) crystallizes in the monoclinic space group C2/c (n° 15), with *a* ~ 7.5, *b* ~ 25, *c* ~ 30 Å, β ~ 93°, *V* ~ 5500 Å³ (see Tables S1 for details). For the heaviest cation containing solids (Rb, Cs), the solvent molecules were located within the pores using low temperature measurement (see Table S3). As a typical illustration, the case of the MIL-141(Cs) structure is described.

The MIL-141(A) structure is built up from tetra-anionic Ni-TCPP⁴⁻ linkers, Fe³⁺ (see below), extra-framework alkali cations and DMF molecules, in agreement with a Fe^{III}(Ni^{II}-TCPP)-A•(DMF)_x (A = Li, Na, K, Rb, Cs; *x* ~ 3) formula. The Fe(III) ion adopts a distorted octahedral coordination (see Table S3 for bond distances) consisting only in oxygen atoms from the carboxylate groups and is connected to four porphyrinic linkers (two chelating and two monodentate carboxylates), acting thus as a slightly distorted tetrahedral node (Figure 1a, bottom). On the organic side, each Ni^{II}-TCPP linker is connected to four Fe(III) ions and acts as a square planar node (Figure 1a, top). Such a resulting arrangement defines a three-dimensional network exhibiting the binodal PtS topology with the inorganic and organic moieties corresponding to S and Pt, respectively (vertexes 4.4.8(2).8(2).8(8).8(8) and 4.4.8(7).8(7).8(7).8(7)). The whole structure ultimately consists of three interpenetrated PtS-type networks, with the porphyrinic rings stacked parallel to each other (Figure 1b). This leads to the formation of two types of channels with free diameters of about 4 and 6 Å containing both the alkali cations and the DMF molecules (Figure 2). On the whole, this structure presents some similarities (especially in term of pore size) with a recently published Cd-based solid,¹²⁸ although this later is built up from a chain of CdO_x polyhedra and trianionic (Pd^{II}-TCPP)H linkers.

The residual electronic density associated with A (i.e., with an intensity being directly related to the weight of the alkali) was found within the porosity not far away from the Fe ions (about 4 to 4.4 Å), close to the 2-fold axis. For the heaviest cations (Rb, Cs), the location of both the DMF molecules and the cation was possible, the latter being disordered over two positions. This positional disorder is also probably effective for the lighter cations (Li, Na, K) but hardly modeled with the available data set. The Cs ion is thus statically distributed on two symmetrically equivalent positions and is surrounded by seven oxygen atoms, five from the porphyrinic linkers (among which two are dangling oxygen atoms from the monodentate carboxylate groups) and two from the DMF molecules, each located in a different channel and pointing toward the cation (see Figure 2a,b). The alkali ions thus lie in the hydrophilic part of the channels, enhancing the

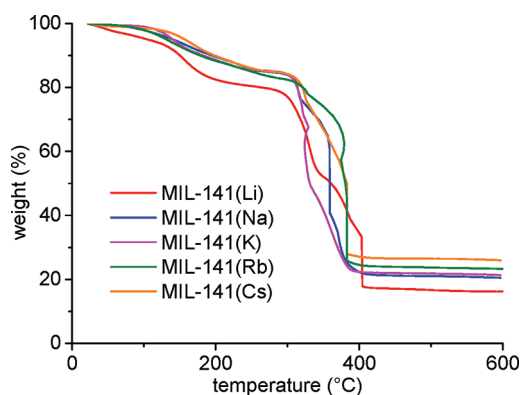


Figure 3. Thermogravimetric analyses of the as-synthesized MIL-141(A) ($A = \text{Li, Na, K, Rb, Cs}$) solids performed under O_2 (heating rate $2\text{ }^\circ\text{C min}^{-1}$).

stability of MIL-141(A) through strong electrostatic interactions between the interpenetrated networks.

Bond valence calculations are in agreement with a +III oxidation state for the Fe cation (see Table S3), which was further confirmed by Mössbauer spectrometry for $A = \text{K, Rb, and Cs}$. Data recorded on the first samples with a large velocity range evidenced the presence of some Fe-based impurities (such as hematite), not detected by X-ray diffraction. Working on the synthesis conditions (amount of base) and the purification step, it was possible to completely discard these impurities which could have resulted from the basic synthetic medium. Data were then collected with a small velocity range to improve the resolution of the hyperfine structure. While in the structures described here, the Fe^{III} ions are on a single crystallographic site, the quadrupolar structure always consists of broadened lines quadrupolar doublets, which could be associated with distortions of the local environment related to the molecules entrapped in the pores, as already observed for other porous Fe-based MOFs (see Figure S6).^{101,102,129} More importantly, the isomer shift values are consistent with the presence of only octahedral high spin Fe^{III} sites. In the case of MIL-141(Li) and MIL-141(Na), the Mössbauer experiments confirmed their limited stability toward humidity which precluded their deeper studies.

Thermal Stability, Structural Flexibility, and Regenerability. Thermogravimetric analysis demonstrated a thermal stability up to $300\text{ }^\circ\text{C}$ under oxygen whatever the alkali cation, a value rather high for a nontrivial ligand, which can be due to the robustness of the porphyrinic core. As shown in Figure 3, the solvents removal occurs between 150 and $250\text{ }^\circ\text{C}$ and represents about 15% of the weight of the starting material, a value consistent with the above-proposed formula (theoretical weight loss 18–19%).

The X-ray thermodiffractometry study, performed under air from 20 to $400\text{ }^\circ\text{C}$, leads to the same conclusion in terms of thermal stability, with the collapse of the solids arising above $300\text{ }^\circ\text{C}$. Nevertheless, at lower temperature, differences emerge depending on the nature of the alkali cation (Figure 4). The departure of the solvent (around 150 – $250\text{ }^\circ\text{C}$) is accompanied by a structural change, which amplitude depends continuously on the size of the cation. For the heaviest cations (Rb, and especially Cs), almost no change in the position of the Bragg peaks is observed. On the opposite, for the lightest cation (Li) severe changes occur. MIL-141(K) presents an intermediate behavior, with a noticeable shift of the Bragg peaks, but to a lesser extent than in MIL-141(Li).

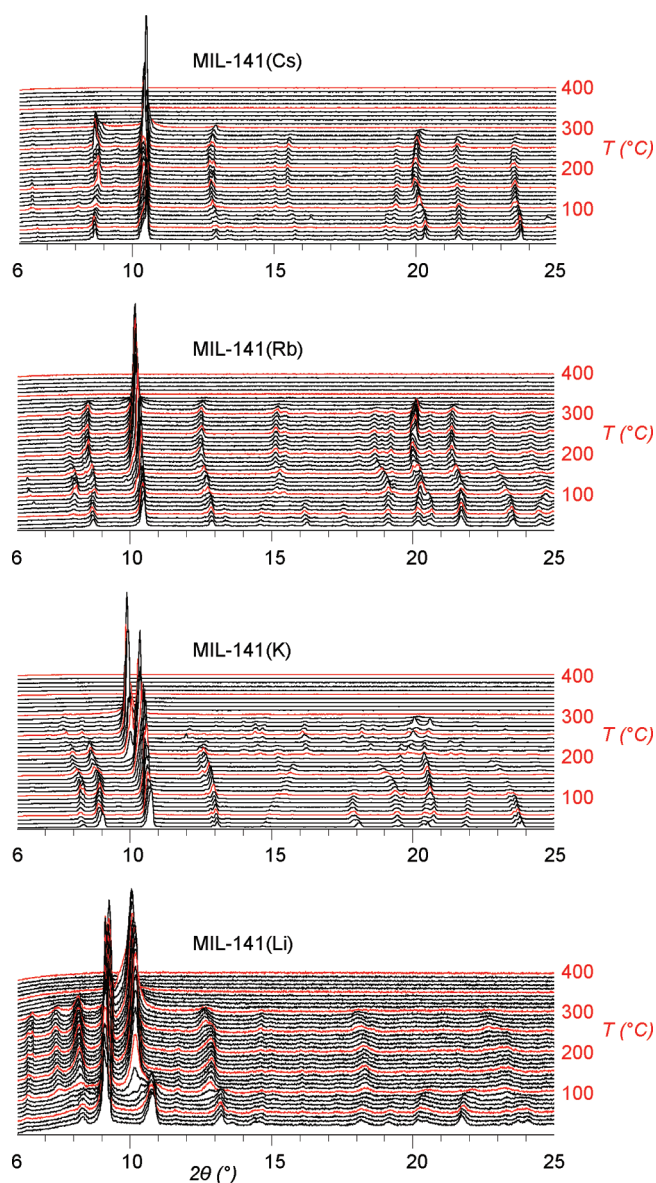


Figure 4. X-ray thermodiffractometry analyses of the as-synthesized MIL-141(A) ($A = \text{Li, K, Rb, Cs}$) solids performed under air from 20 to $400\text{ }^\circ\text{C}$ ($10\text{ }^\circ\text{C}$ step, $\lambda_{\text{CoK}\alpha} = 1.7890\text{ \AA}$). Red patterns are associated with $T = 50, 100, 150, 200, 250, 300, 350,$ and $400\text{ }^\circ\text{C}$.

In order to assess the reversibility of this transformation, the as-synthesized solids were heated up to $250\text{ }^\circ\text{C}$ and cooled down to room temperature, and this cycle was again repeated. As shown in Figure 5 for $A = \text{Li, Cs}$ (see Figure S3 for the other cations), when the sample is cooled down to room-temperature a structure change occurs probably associated with rehydration, here also more or less marked depending on the size of the alkali cation. This new structural form associated with an adsorption of water in the desolvated form of MIL-141(A) confirms the presence of a slight flexibility of the structure upon adsorption. When the solids are heated up again to $250\text{ }^\circ\text{C}$, they recover their high-temperature (HT) structural forms for $A = \text{K, Rb, Cs}$, indicating that the transformation is reversible. At first sight, the phenomenon seems irreversible for $A = \text{Li}$. Nevertheless, the transformation is reversible for a third cycle (see Figure S4), indicating that the first observation could be related to a slower kinetics of desolvation for MIL-141(Li).

The flexible character of MIL-141(A) upon solvent departure might arise, either from a distortion of each interpenetrated network or a global sliding of the networks, leading to a change of the pore size or at least of the shape of its hydrophilic part. The alkali cation may counterbalance this effect and even completely prevent the flexibility as for the largest one (Cs). Preliminary examination of the MIL-141(Cs) solid indeed showed that the unit-cell of the HT form (monoclinic $C2/c$, $a = 7.291(1)$, $b = 24.182(4)$, $c = 30.860(4)$ Å, $\beta = 92.26(1)^\circ$, $V = 5437(1)$ Å³, see Figure S5) is very similar to the one of the as-synthesized solid (monoclinic $C2/c$, $a = 7.360(1)$, $b = 24.792(1)$, $c = 29.743(2)$ Å, $\beta = 94.44(1)^\circ$, $V = 5410.8(5)$ Å³, $\Delta(a,b,c) < 3.7\%$), whereas a significant decrease of the shortest crystallographic parameter (>6%) is observed for MIL-141(K) (HT form: orthorhombic $C222_1$, $a = 25.877(1)$, $b = 6.762(1)$, $c = 31.986(1)$ Å, $V = 5596.9(1)$ Å³, see Figure S5; as-synthesized form: monoclinic $C2/c$, $a = 7.228(4)$, $b = 25.00(2)$, $c = 30.90(2)$

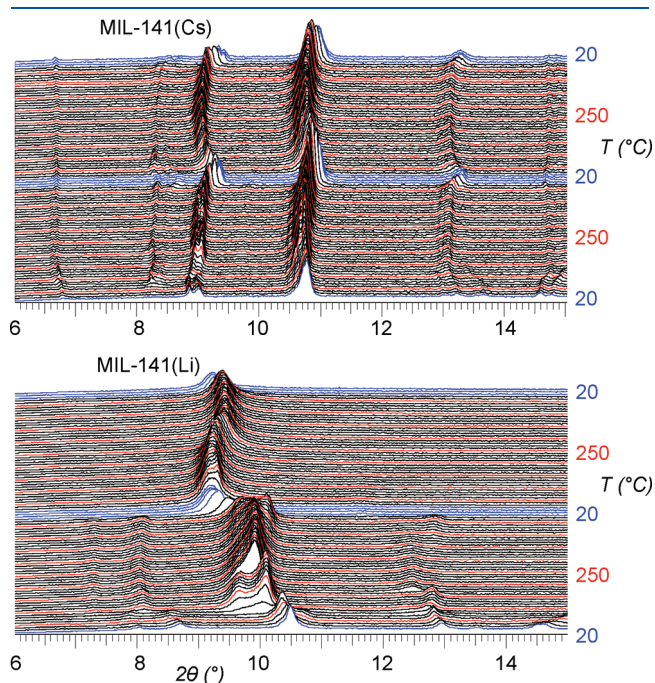


Figure 5. X-ray thermodiffractometry analyses of the as-synthesized MIL-141(A) (A = Li, Cs) solids performed under air, using the following thermal cycle: 20 to 250 °C to 20 °C to 250 °C to 20 °C (10 °C step, $\lambda_{\text{CoK}\alpha} = 1.7890$ Å).

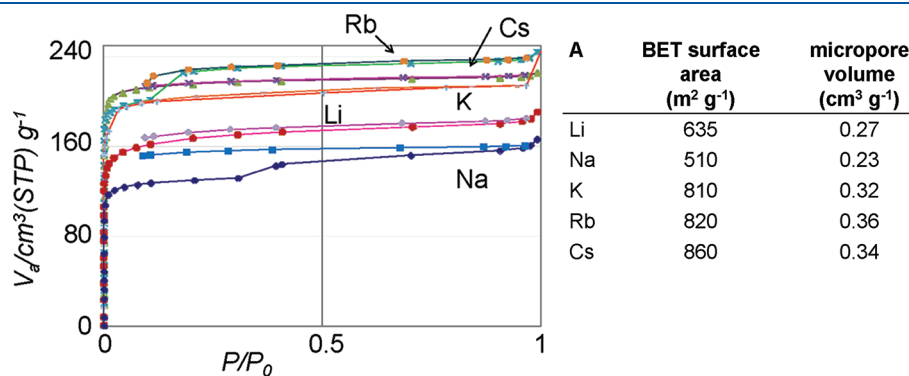


Figure 6. Nitrogen sorption isotherms measured at 77 K for MIL-141(A) (A = Li, Na, K, Rb, Cs) together with the corresponding BET surface areas and micropore volumes.

Å, $\beta = 93.17(1)^\circ$, $V = 5575(6)$ Å³). As illustrated in Figure S1, the shortening of the corresponding cell parameter corresponds to a decrease of the Fe•••A•••Fe distance. In order to balance the lack of oxygen atoms within its coordination sphere resulting from the departure of the DMF molecules, the alkaline ion A may need to get closer to the oxygen atoms of the framework (O_{fr}), i.e. to the carboxylate surrounding the Fe ion. This effect would be more pronounced for the smallest alkaline ions (which require shorter A••• O_{fr} distances) than for the largest ones, leading to more pronounced structural changes when the size of the cation decreases. One can still note that this flexibility is associated with rather low amplitudes of breathing compared to other classes of highly flexible MOFs^{130,131} (displacement of the main Bragg peak (022) of about 0.3 Å for MIL-141(Li)).

Adsorption Properties. The porosity of the MIL-141(A) (A = Li, Na, K, Rb, Cs) solids was first investigated by nitrogen sorption at 77 K. Prior to the measurement, the as-synthesized solids were activated under vacuum at 170 °C in order to evacuate the DMF molecules from the pores. Temperature dependent infra-red spectroscopy (see Figure S12 for A = K) confirmed the full departure of the solvent using this condition, without any alteration of the framework. The N₂ sorption isotherms are illustrated in Figure 6, together with the deduced BET surface areas and micropore volumes extracted from the t -plot analyses. All MIL-141(A) solids are microporous solids with a reasonably high surface area ($S_{\text{BET}} \sim 500\text{--}860$ m² g⁻¹) and with slight changes in the total adsorption capacity (160–240 cm³ (STP) g⁻¹). Interestingly, the shape of the isotherms depends on the nature of the cation A. Especially, steps were observed when the isotherms are plotted in log-scale both at low (see Figure S7) and intermediate pressures. Whereas the first ones are not surprising in microporous solids and could be assigned to the existence of specific adsorption sites, those present at intermediate pressure are less common and could be attributed to the structural flexibility of the framework. The reproducibility of these steps was checked on different batches (see Figure S8 for A = Rb), supporting the fact that these behaviors are intrinsic to the materials and not related to activation issues. This behavior is consistent with the structural observation presented above, suggesting that the MIL-141 compounds are rather flexible solids. As a consequence and contrary to the case of rigid solids such as zeolites, the total pore volume and surface area do not directly decrease with the mass of the alkali ion, as they rely both on the initial pore opening (which is dependent on A, see above) and the structural flexibility. One can even note the concomitant decrease of the surface area and

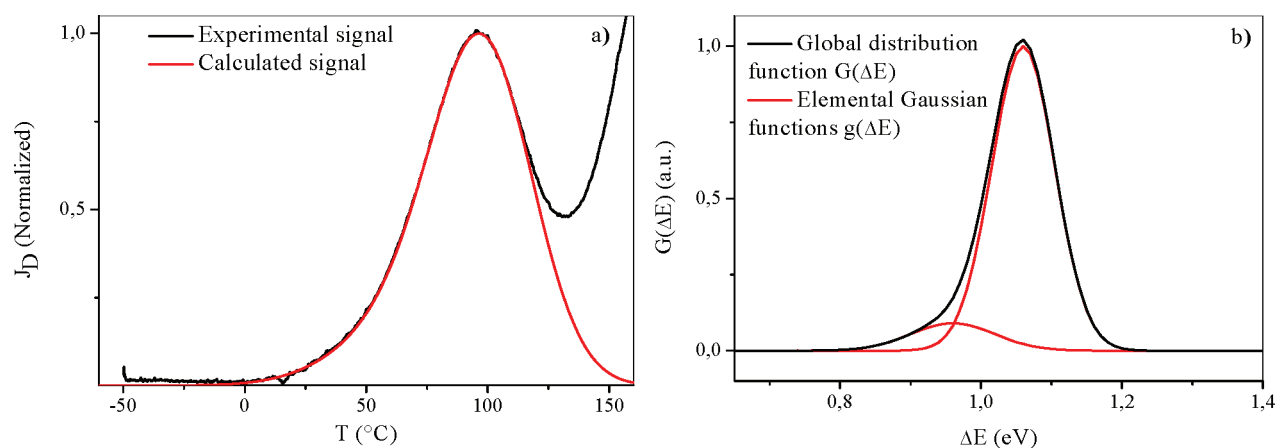


Figure 7. TSC analysis of MIL-141(Rb). a) Comparison between the calculated (black line) and the experimental (red line) normalized depolarization current and b) line shape of the normalized distribution function $G(\Delta E)$ used for the calculation of $J_D(T)$. Black and red lines represent the global $G(\Delta E)$ and its decomposition into two elementary Gaussian functions $g(\Delta E)$, respectively.

the size of the cation, what could at first sight appear inconsistent. This result can nevertheless be understood in light of the thermal analysis: the solvent departure is accompanied by a shrinkage of the pores, but this effect is counterbalanced by the presence of bulkier cations which prevents this pore closure, thus lead to higher sorption capacities than the smaller cations. This phenomenon was in fact already observed in the flexible Fe(III) terephthalate MIL-53, in which the introduction of bulky perfluoro groups on the linker lead to a significant increase of the permanent microporosity.¹⁰¹ Theoretical accessible surface area and micropore volume were estimated for the activated MIL-141(Cs) using the method published elsewhere (see the Supporting Information for details).¹³² This calculation leads to values of $605 \text{ m}^2 \text{ g}^{-1}$ and $0.39 \text{ cm}^3 \text{ g}^{-1}$, respectively. The good agreement between the theoretical and experimental micropore volumes for A = Cs not only attests the effectiveness of the activation procedure but also confirms once again that the structural changes occurring upon solvent removal do not drastically affect the pore size/volume for this bulky cation. The discrepancy observed for the surface area is not unexpected and could simply arise from the fact that the BET model, although commonly used, is known to be not relevant for microporous solids.¹³³ For the lightest cations (Li, Na), the experimental pore volumes remain lower than the calculated ones, in agreement with the contraction of the pores proposed above. Finally, the stability of the framework toward successive adsorption/desorption cycles was tested: as shown in Figure S9, no change in the adsorption isotherm was observed for MIL-141(Rb), assessing the robustness of this solid.

As already mentioned in the Introduction and recently highlighted by Hupp and co-workers,⁸⁹ examples of stable MOFs based on porphyrin derivatives and presenting a permanent microporosity (especially toward nitrogen) are scarce.^{70,73–75,86–88,134} The MIL-141(A) thus represents an appealing series of porous coordination polymers based on a porphyrin derivative, presenting reasonably high BET surface area and exhibiting two types of potentially accessible cation sites, either intra- (Ni) or inter- (A) framework. The following section is devoted to the characterization of the extra-framework cation sites.

Characterization of the Extra-Framework Cation Sites: Thermally Stimulated Current (TSC) Measurements. A detailed description of the TSC technique and analysis methods

used in this work can be found in the literature^{135,136} and is briefly reminded in the Supporting Information. The TSC spectroscopy addresses the local dynamic of charges, basically by measuring the depolarization current J_D , when a dipolar solid, which was first polarized and frozen, returns to the equilibrium state, under a controlled heating ramp. Applied to ionic solids, the dielectric response can be regarded as arising from the dipolar reorientation associated with the ionic charge hopping over short distances. Based on the data previously reported on aluminosilicate compounds (zeolites or clay minerals),^{137–141} the dielectric relaxation responses of MIL-141(A) are expected to arise from the relaxation of the alkali cation, which can be regarded as the reorientation of the dipoles, constituted by the cations A and their surrounding oxygen atoms of the framework. By fitting the depolarization current J_D with an appropriate function (see the SI), TSC gives access to the distribution function $G(\Delta E)$. One can further extract the partition of the extra-framework cations among their possible hosting sites and the distribution of the activation energies associated with the relaxation of the cation in their sites: this latter information allowing us to get an indirect evaluation of the interaction between the A cations and their surrounding environment (here the framework).

Figure 7a illustrates a typical example of the TSC signal, obtained for the activated MIL-141(Rb) sample. $J_D(T)$ exhibits a broad peak, accompanied by a sudden increase of the signal at high temperature. This later response corresponds to the space charge effect, which results from the accumulation of ionic charges at the sample/insulator layer interface.¹⁴² One should notice that it is not an intrinsic dielectric relaxation phenomenon and hence must not be taken into account in the experimental data analysis. The good agreement between the experimental and calculated signals was thus achieved by considering the distribution function of the activation energies $G(\Delta E)$ depicted in Figure 7b. As observed, $G(\Delta E)$ appears as a contribution of two Gaussian functions, centered around two distinct mean values of ΔE , which suggests the presence of two dipole populations. Similarly to zeolites,^{137,139,140} this result indicates that the Rb^+ ions are distributed over two types of sites in the activated MIL-141(Rb) solid.

Further, considering the relative area of each Gaussian function (see Table 1), one can access the relative population of both families of cation sites. The Rb^+ extra-framework cations

Table 1. Parameters of $G(\Delta E_i)$ Determined from the Fit of the Experimental TSC Signal with Eq 2 (See the Supporting Information), Assuming That $G(\Delta E_i)$ Is the Summation of Two Gaussian Functions $g_i(\Delta E)^a$

solid	$g_1(\Delta E)$		$g_2(\Delta E)$		$\overline{\Delta E}$ (eV)
	ΔE (eV)	Occ. (%)	ΔE (eV)	Occ. (%)	
MIL-141(Li)	0.85	44	0.95	56	0.91
MIL-141(Na)	0.84	11	0.95	89	0.94
MIL-141(K)	0.86	5	0.96	95	0.96
MIL-141(Rb)	0.96	11	1.06	89	1.05
MIL-141(Cs)	1.11	13	1.17	87	1.16

^a ΔE (± 0.02 eV) is the energy value at the Gaussian maximum and "Occupancy" is the area relative to the global distribution function $G(\Delta E_i)$. $\overline{\Delta E}$ (± 0.02 eV) represents the mean energy associated to the relaxation of the alkali cation in the porous structure.

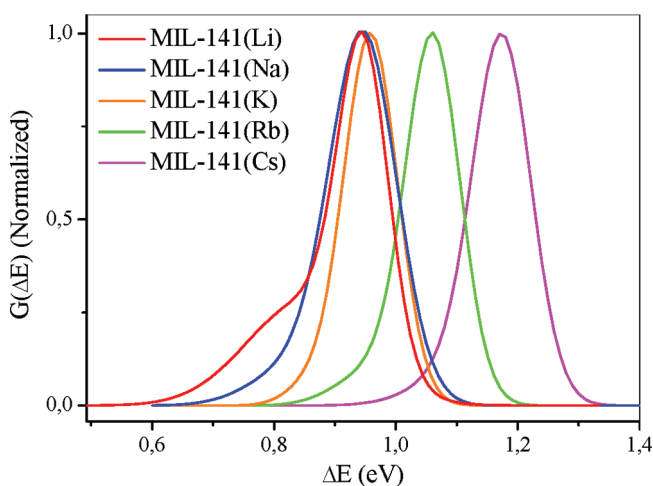


Figure 8. Alkali cation dependence of the $G(\Delta E)$ distributions of MIL-141(A) (A = Li, Na, K, Rb, Cs) solids.

are predominantly localized on a single site, the second one being occupied by only a very small fraction of these cations (proportion of 11%). Following the same analysis procedure, similar results are obtained for the other MIL-141 solids (see Table 1). This indicates that in the activated forms of MIL-141(A) (A = Na, K, Rb, Cs), most of the cations are preferentially located in one type of site, similarly to what happens in the as-synthesized form (see structural analysis above), although a rearrangement upon solvent departure could not be *a priori* totally excluded. This behavior strongly deviates with those usually observed in other microporous systems such as zeolites, wherein several types of cationic sites are present.^{113–116}

Further, the situation drastically differs for the MIL-141(Li) phase with Li cations roughly equally distributed into two sites. This fact could be related with the higher structural flexibility of MIL-141(Li) (see above) and to the smaller size of this cation, which may allow it to access specific sites not available for larger ones. Nevertheless, the rather low stability of this particular solid (see above) precludes a deeper analysis for drawing a definitive conclusion.

Figure 8 compiles the $G(\Delta E)$ obtained for all the MIL-141(A) solids. It is observed that the position of $G(\Delta E)$ depends on the nature of A, as shown by the signal shift toward the highest

energy domain when the alkali size increases. One can further extract from these plots the mean energy value ($\overline{\Delta E}$) for all the investigated cations that represents the most probable detrapping energy of the A cation from its initial site. Such energy is related to the strength of the A/framework interaction, assuming that the more difficult the extraction of the cation is, the stronger the A/framework interaction is. The increase of the detrapping energy with the cation size as reported in Table 1 suggests that the interaction energy between the alkali ion and the surrounding oxygen atoms of the framework becomes stronger from Li to Cs. This energy sequence cannot be directly compared to the one observed in zeolites, since in this later case, different evolutions can be observed depending both on the Si/Al ratio and the topology of the aluminosilicates.^{137–140} However, one may note that the interaction energy between the alkali ion and the framework is usually higher for the MIL-141(A) solids than those encountered in zeolites (as an example $\overline{\Delta E} = 0.8$ and 0.6 eV in NaY and NaX faujasites, respectively¹³⁷). This is confirmed by preliminary CO adsorption *in situ* IR experiments, which showed that the polarizing ability of the Li and Na cations is far less marked in MIL-141 than in the corresponding Y and X zeolites (see Figure S13). One can thus expect a different behavior of this material compared to zeolites with respect to adsorption/separation processes which are known to be governed by the cation/adsorbate interactions, as in the case for the O₂/N₂ mixtures.

Adsorption Properties of MIL-141(A) with Respect to the Single Gases O₂ and N₂. Gas separation and especially oxygen/nitrogen separation from air are of proven commercial importance, for example oxygen finding a wide variety of use in industries (steel, paper, and pulp industries; glass-melting furnaces and also chemical processes such as biological treatment of wastewater). For high-volume production, the cryogenic distillation of liquefied air is employed, whereas for low or medium volume production, air separation by membrane separation or vacuum/pressure swing adsorption processes (V/PSA)¹⁴³ are found to be more economically viable. Porous carbons have been shown to be efficient for nitrogen production, with a separation based on kinetics (diffusion limited behavior).^{144–150} Alternatively, for oxygen production, zeolites can be used, and, in this case, separation occurs through the preferential adsorption of one constituent.¹⁵¹ Especially, alkali containing X Faujasite-type zeolites present a highly selective adsorption of N₂ toward O₂. This effect was shown to be related to the polarizing power of the extra-framework cations and thus to be dependent on the number (ratio Si/Al) and the nature of the entrapped cation.^{152,153} Especially, the LiLSX zeolite (ratio Si/Al = 1) presents the strongest Li⁺•••N₂ interaction leading to the highest N₂/O₂ selectivity.^{123,154}

Adsorption of N₂ and O₂ at 30 °C up to 40 bar in MIL-141(A) was thus investigated for A = Li, K, Cs. A detailed description of the gravimetric installation, the experimental procedure, and the measurement accuracy used in this work can be found in the literature.¹⁵⁵ The resulting isotherms are all of I-type, with a slope at the initial stage of adsorption and a saturation capacity both depending on the pair gas/cation (Figure 9). Whatever the cation considered and contrary to the case of the LSX zeolites, all solids adsorb preferentially O₂ toward N₂, both at low (see Figure S10) and high pressures (Figure 9). The resulting N₂/O₂ selectivities calculated at 4 bar for air (gas composition 80% N₂ and 20% O₂) (see the Supporting Information) are estimated to be 0.73, 0.87, and 1.0 for MIL-141(A) with A = Li, K,

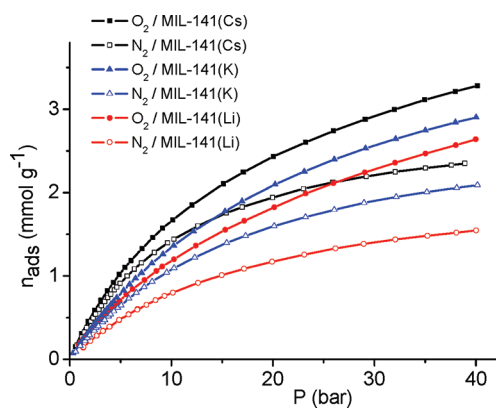


Figure 9. Nitrogen and oxygen sorption isotherms measured at 303 K for MIL-141(A) (A = Li, K, Cs).

Cs, respectively. They strongly differ with those obtained for the LSX-Faujasite (5.25, 3.33, and 1.99 for Li, Na and K, respectively).¹⁵⁴ One can thus note that, whereas the N_2/O_2 selectivity increases when the size of A decreases for ALSX, the opposite is observed for MIL-141(A), with an increase of the O_2/N_2 selectivity.

All these results suggest that in MIL-141(A), the alkali ions are not as strong adsorption sites for N_2 as they are in zeolites. This could be related to the main conclusions of the TSC and IR studies. Indeed, in MIL-141(A), A interacts more strongly with the framework than in the zeolite, leading to weaker interactions with N_2 . Above a lower affinity for N_2 , we also observe an inversion of selectivity, especially at high pressure. This could not be related to size effects (see the sorption isotherms of N_2 at 77 K in Figure 6) but most probably to the presence of selective adsorption sites for oxygen, typically the macrocyclic linkers. Indeed, transition metal macrocyclic compounds as porphyrins are well-known to interact with O_2 , and a number of such systems have been studied for catalytic applications implying O_2 , such as oxygen reduction reactions.^{156,157} Depending on their nature, the metal or the organic substituents (especially electron rich substituents¹⁵⁸) may strengthen both the metal- O_2 ¹⁵⁹ or macrocycle- O_2 ¹⁶⁰ interactions. Based on this idea, porous membranes incorporating Co(II) porphyrins were indeed already used for O_2/N_2 separation: they were shown to adsorb preferentially O_2 over N_2 because of the strong interaction between O_2 and the Co(II) centers¹⁶¹ and finally present good O_2/N_2 separation abilities, the Co(II) centers favoring the transportation of O_2 through a jump mechanism.^{158,161–163} Based on this knowledge, one can suggest that the ligands may finally here play the key role as O_2 -specific adsorption sites and give rise to the same inversed selectivity. The effect is still less pronounced in MIL-141 than in the aforementioned membranes simply because Ni(II) porphyrins are less prone to interact with axial ligands (here O_2) than their Co(II) counterpart.¹⁵⁹ From an adsorption point of view, the MIL-141 series seems thus to behave more like MOFs presenting coordinatively unsaturated transition-metal sites (interacting specifically with O_2)^{120,122} rather than cationic zeolites. Nevertheless, deeper *in situ* IR experiments are needed to fully prove this assertion.

CONCLUSION

We report here a series of iron(III)-based MOFs (MIL-141(A), A = Li, Na, K, Rb, Cs) built up from a porphyrinic

linker, with the presence of alkali ions within the pores. All solids are stable upon solvent removal and present a significant permanent porosity, a rare property in the area of porphyrin-based coordination polymers. Alkali cations have a noticeable effect on the structural flexibility of the solid, its rigidity increasing with the cation size. TSC measurements revealed that the major part of the cations (Na, K, Rb, Cs) are still located in one hosting site after the activation procedure. The cations/framework interactions are stronger here than in analogous cation-containing zeolites leading to a lower N_2 /extra-framework interaction and thus to a reverse N_2 over O_2 selectivity, that can also be explained by a preferential adsorption of O_2 over the porphyrinic linkers. These solids finally combine three cationic species: the node (Fe^{3+}), the porphyrin central metal (Ni^{2+}), and the extra-framework cation entrapped within the pores (A^+) among which two may act as coordinatively unsaturated metal sites (Ni^{2+} and A^+). The extension of their chemical composition (especially playing with these two cations) as well as the presence of one cation hosting site and the preferred adsorption of O_2 , appear promising for further catalytic applications^{89,128,164} implying oxygen reactivity or bi-site catalysis as well as for specific properties in the area of gas separation. Such work is currently in progress.

ASSOCIATED CONTENT

S Supporting Information. Full experimental details (synthesis, characterization, XRD data, structural description, simulation methodology, CIF files). This material is available free of charge via the Internet at <http://pubs.acs.org>.

AUTHOR INFORMATION

Corresponding Author

*E-mail: devic@chimie.uvsq.fr.

ACKNOWLEDGMENT

The authors acknowledge the financial support of the French ANR 'CONDMOFS' (ANR-07-BLAN-1-203677), C. Thouvenot for her technical assistance (synthesis and EDX analysis), Dr. F. Nouar and Dr. J. Eubank for their help with TOPOS, the ESRF for providing beamtime, and Dr. Y. Filinchuk for his assistance. Dr. S. Wuttke acknowledges Alexander von Humboldt foundation for his fellowship.

REFERENCES

- (1) See for example the special issue. *Chem. Soc. Rev.* **2009**, 38, 1201–1507 and references therein.
- (2) Zhao, D.; Timmons, D. J.; Yuan, D.; Zhou, H.-C. *Acc. Chem. Res.* **2011**, 44, 123–133.
- (3) Zou, Y.; Park, M.; Hong, S.; Lah, M. S. *Chem. Commun.* **2008**, 2340–2342.
- (4) Chen, Z.; Xiang, S.; Liao, T.; Yang, Y.; Chen, Y.-S.; Zhou, Y.; Zhao, D.; Chen, B. *Cryst. Growth Des.* **2010**, 10, 2775–2779.
- (5) Zheng, B.; Liang, Z.; Li, G.; Huo, Q.; Liu, Y. *Cryst. Growth Des.* **2010**, 10, 3405–3409.
- (6) Vagin, S. I.; Ott, A. K.; Hoffmann, S. D.; Lanzinger, D.; Rieger, B. *Chem.—Eur. J.* **2009**, 15, 5845–5853.
- (7) Zhao, X.; He, H.; Hu, T.; Dai, F.; Sun, D. *Inorg. Chem.* **2009**, 48, 8057–8059.
- (8) Humphrey, S. M.; Oungoulian, S. E.; Yoon, J. W.; Hwang, Y. K.; Wise, E. R.; Chang, J.-S. *Chem. Commun.* **2008**, 2891–2893.

- (9) Farha, O. K.; Malliakas, C. D.; Kanatzidis, M. G.; Hupp, J. T. *J. Am. Chem. Soc.* **2009**, *132*, 950–952.
- (10) Lambert, J. B.; Liu, Z.; Liu, C. *Organomet.* **2008**, *27*, 1464–1469.
- (11) Vagin, S.; Ott, A.; Weiss, H.-C.; Karbach, A.; Volkmer, D.; Rieger, B. *Eur. J. Inorg. Chem.* **2008**, *16*, 2601–2609.
- (12) Liu, X.; Park, M.; Hong, S.; Oh, M.; Yoon, J. W.; Chang, J.-S.; Lah, M. S. *Inorg. Chem.* **2009**, *48*, 11507–11509.
- (13) Tsai, C.-C.; Luo, T.-T.; Yin, J.-F.; Lin, H.-C.; Lu, K.-L. *Inorg. Chem.* **2009**, *48*, 8650–8652.
- (14) Wenzel, S. E.; Fischer, M.; Hoffmann, F.; Frolba, M. *Inorg. Chem.* **2009**, *48*, 6559–6565.
- (15) Wu, S.; Ma, L.; Long, L.-S.; Zheng, L.-S.; Lin, W. *Inorg. Chem.* **2009**, *48*, 2436–2442.
- (16) Das, S.; Kim, H.; Kim, K. *J. Am. Chem. Soc.* **2009**, *131*, 3814–3815.
- (17) Higuchi, M.; Tanaka, D.; Horike, S.; Sakamoto, H.; Nakamura, K.; Takashima, Y.; Hijikata, Y.; Yanai, N.; Kim, J.; Kato, K.; Kubota, Y.; Takata, M.; Kitagawa, S. *J. Am. Chem. Soc.* **2009**, *131*, 10336–10337.
- (18) Schnobrich, J. K.; Lebel, O.; Cychosz, K. A.; Dailly, A.; Wong-Foy, A. G.; Matzger, A. J. *J. Am. Chem. Soc.* **2010**, *132*, 13941–13948.
- (19) Swamy, S. I.; Bacsa, J.; Jones, J. T. A.; Stylianou, K. C.; Steiner, A.; Ritchie, L. K.; Hasell, T.; Gould, J. A.; Laybourn, A.; Khimiyak, Y. Z.; Adams, D. J.; Rosseinsky, M. J.; Cooper, A. I. *J. Am. Chem. Soc.* **2010**, *132*, 12773–12775.
- (20) Yuan, D.; Zhao, D.; Sun, D.; Zhou, H.-C. *Angew. Chem., Int. Ed.* **2010**, *49*, 5357–5361.
- (21) Wang, X. S.; Ma, S.; Sun, D.; Parkin, S.; Zhou, H. C. *J. Am. Chem. Soc.* **2006**, *128*, 16474–16475.
- (22) Furukawa, H.; Ko, N.; Go, Y. B.; Aratani, N.; Choi, S. B.; Choi, E.; Yazaydin, A. O.; Snurr, R. Q.; O’Keeffe, M.; Kim, J.; Yaghi, O. M. *Science* **2010**, *329*, 424–428.
- (23) Kesanli, B.; Cui, Y.; Smith, M. R.; Bittner, E. W.; Bockrath, B.; Lin, W. *Angew. Chem., Int. Ed.* **2005**, *44*, 72–75.
- (24) Lin, X.; Jia, J.; Zhao, X.; Thomas, K. M.; Blake, A. J.; Walker, G. S.; Champness, N. R.; Hubberstey, P.; Schröder, M. *Angew. Chem., Int. Ed.* **2006**, *45*, 7358–7364.
- (25) Farha, O. K.; Yazaydin, A. O.; Eryazici, I.; Malliakas, C. D.; Hauser, B. G.; Kanatzidis, M. G.; Nguyen, S. T.; Snurr, R. Q.; Hupp, J. T. *Nat. Chem.* **2010**, *2*, 944–948.
- (26) Baudron, S. A.; Hosseini, M. W. *Inorg. Chem.* **2006**, *45*, 5260–5262.
- (27) Constable, E. C.; Dunphy, E. L.; Housecroft, C. E.; Neuburger, M.; Schaffner, S.; Schaper, F.; Batten, S. R. *Dalton Trans.* **2007**, 4323–4332.
- (28) Halper, S. R.; Do, L.; Stork, J. R.; Cohen, S. M. *J. Am. Chem. Soc.* **2006**, *128*, 15255–15268.
- (29) Kitaura, R.; Onoyama, G.; Sakamoto, H.; Matsuda, R.; Noro, S.; Kitagawa, S. *Angew. Chem., Int. Ed.* **2004**, *43*, 2684–2687.
- (30) Wu, C. D.; Hu, A.; Zhang, L.; Lin, W. *J. Am. Chem. Soc.* **2005**, *127*, 8940–8941.
- (31) D’Souza, F.; Maligaspe, E.; Ohkubo, K.; Zandler, M. E.; Subbaiyan, N. K.; Fukuzumi, S. *J. Am. Chem. Soc.* **2009**, *131*, 8787–8797.
- (32) Suslick, K. S.; Watson, R. A.; Wilson, S. R. *Inorg. Chem.* **1991**, *30*, 2311–2317.
- (33) Suslick, K. S.; Watson, R. A. *New J. Chem.* **1992**, *16*, 633–642.
- (34) Maldotti, A.; Amadelli, R.; Bartocci, C.; Carassiti, V.; Polo, E.; Varani, G. *Coord. Chem. Rev.* **1993**, *125* (1–2), 143–154.
- (35) Wittmer, L. L.; Holten, D. *J. Phys. Chem.* **1996**, *100*, 860–868.
- (36) Donker, H.; Koehorst, R. B. M.; Schaafsma, T. J. *J. Phys. Chem. B* **2005**, *109*, 17031–17037.
- (37) Takagi, S.; Eguchi, M.; Tryk, D. A.; Inoue, H. *J. Photochem. Photobiol., C.* **2006**, *7* (2–3), 104–126.
- (38) Bhyrappa, P.; Sankar, M.; Varghese, B. *Inorg. Chem.* **2006**, *45*, 4136–4149.
- (39) Kadish, K. M.; Lin, M.; Van Caemelbecke, E.; De Stefano, G.; Medforth, C. J.; Nurco, D. J.; Nelson, N. Y.; Krattinger, B.; Muzzi, C. M.; Jaquinod, L.; Xu, Y.; Shyr, D. C.; Smith, K. M.; Shelnutt, J. A. *Inorg. Chem.* **2002**, *41*, 6673–6687.
- (40) Kadish, M.; Van Caemelbecke, E. *J. Solid State Electrochem.* **2003**, *7* (5), 254–258.
- (41) Lash, T. D.; Hayes, M. J.; Spence, J. D.; Muckey, M. A.; Ferrence, G. M.; Szczepura, L. F. *J. Org. Chem.* **2002**, *67*, 4860–4874.
- (42) Richeter, S.; Jeandon, C.; Gisselbrecht, J. P.; Ruppert, R.; Callot, H. J. *J. Am. Chem. Soc.* **2002**, *124*, 6168–6179.
- (43) Singh, P.; Das, A. K.; Sarkar, B.; Niemeyer, M.; Roncaroli, F.; Olabe, J. A.; Fiedler, J.; Zalis, S.; Kaim, W. *Inorg. Chem.* **2008**, *47*, 7106–7113.
- (44) Sun, H. R.; Smirnov, V. V.; DiMagno, S. G. *Inorg. Chem.* **2003**, *42*, 6032–6040.
- (45) Winters, M. U.; Dahlstedt, E.; Blades, H. E.; Wilson, C. J.; Frampton, M. J.; Anderson, H. L.; Albinsson, B. *J. Am. Chem. Soc.* **2007**, *129*, 4291–4297.
- (46) Ricard, D.; L’Her, M.; Richard, P.; Boitrel, B. *Chem.—Eur. J.* **2001**, *7*, 3291–3297.
- (47) Spasojevic, I.; Batinic-Haberle, I. *Inorg. Chim. Acta* **2001**, *317* (1–2), 230–242.
- (48) Collman, J. P.; Kaplun, M.; Sunderland, C. J.; Boulatov, R. *J. Am. Chem. Soc.* **2004**, *126*, 11166–11167.
- (49) Carlsen, C. U.; Moller, J. K. S.; Skibsted, L. H. *Coord. Chem. Rev.* **2005**, *249* (3–4), 485–498.
- (50) Liu, J. G.; Naruta, Y.; Tani, F. *Angew. Chem., Int. Ed.* **2005**, *44*, 1836–1840.
- (51) Mackintosh, H. J.; Budd, P. M.; McKeown, N. B. *J. Mater. Chem.* **2008**, *18*, 573–578.
- (52) Shinokubo, H.; Osuka, A. *Chem. Commun.* **2009**, 1011–1021.
- (53) Collman, J. P.; Lee, V. J.; Kellen-Yuen, C. J.; Zhang, X.; Ibers, J. A.; Brauman, J. I. *J. Am. Chem. Soc.* **1995**, *117*, 692–703.
- (54) Perollier, C.; Pecaut, J.; Ramasseul, R.; Marchon, J. C. *Inorg. Chem.* **1999**, *38*, 3758.
- (55) Veyrat, M.; Maury, O.; Faverjon, F.; Over, D. E.; Ramasseul, R.; Marchon, J.-C.; Turowska-Tyrk, I.; Scheidt, W. R. *Angew. Chem., Int. Ed.* **1994**, *33*, 220–223.
- (56) Geier, G. R.; Ciringh, Y.; Li, F. R.; Haynes, D. M.; Lindsey, J. S. *Org. Lett.* **2000**, *2*, 1745–1748.
- (57) Geier, G. R.; Lindsey, J. S. *Tetrahedron* **2004**, *60* (50), 11435–11444.
- (58) Lindsey, J. S.; Schreiman, I. C.; Hsu, H. C.; Kearney, P. C.; Marguerettaz, A. M.; Rothemund, J. *Org. Chem.* **1987**, *52*, 827–836.
- (59) Dalton, J.; Milgrom, L. R.; Pemberton, S. M. *J. Chem. Soc., Perkin Trans. 2* **1980**, 370–372.
- (60) Phillippi, M. A.; Shimomura, E. T.; Goff, H. M. *Inorg. Chem.* **1981**, *20*, 1322–1325.
- (61) Steene, E.; Halvorsen, I.; Nilsen, H. J.; Lie, R.; Ghosh, A.; Guo, N.; Kadish, K. M. *Abstr. Pap. Am. Chem. Soc.* **2000**, *219*, 569–569.
- (62) Imahori, H.; Hosomizu, K.; Mori, Y.; Sato, T.; Ahn, T. K.; Kim, S. K.; Kim, D.; Nishimura, Y.; Yamazaki, I.; Ishii, H.; Hotta, H.; Matano, Y. *J. Phys. Chem. B* **2004**, *108*, 5018–5025.
- (63) Hosomizu, K.; Oodoi, M.; Umeyama, T.; Matano, Y.; Yoshida, K.; Isoda, S.; Isosomppi, M.; Tkachenko, N. V.; Lemmetyinen, H.; Imahori, H. *J. Phys. Chem. B* **2008**, *112*, 16517–16524.
- (64) Bezzu, C. G.; Helliwell, M.; Warren, J. E.; Allan, D. R.; McKeown, N. B. *Science* **2010**, *327*, 1627–1630.
- (65) Spitler, E. L.; Dichtel, W. R. *Nature Chem.* **2010**, *2*, 672–677.
- (66) Chen, L.; Yang, Y.; Jiang, D. *J. Am. Chem. Soc.* **2010**, *132*, 9138–9143.
- (67) Kühn, E.; Bulach, V.; Hosseini, M. W. *Chem. Commun.* **2008**, 5104–5106.
- (68) Abrahams, B. F.; Hoskins, B. F.; Michail, D. M.; Robson, R. *Nature* **1994**, *369*, 727–729.
- (69) Lin, K.-J. *Angew. Chem., Int. Ed.* **1999**, *38*, 2730–2732.
- (70) Suslick, K. S.; Bhyrappa, P.; Chou, J.-H.; Kosal, M. E.; Nakagaki, S.; Smithenry, D. W.; Wilson, S. R. *Acc. Chem. Res.* **2005**, *38*, 283–291.
- (71) Goldberg, I. *CrystEngComm* **2008**, *10*, 637–645.
- (72) DeVries, L. D.; Choe, W. *J. Chem. Crystallogr.* **2009**, *39*, 229–240.
- (73) Ohmura, T.; Usuki, A.; Fukumori, K.; Ohta, T.; Ito, M.; Tatsumi, K. *Inorg. Chem.* **2006**, *45*, 7988–7990.

- (74) Shultz, A. M.; Farha, O. K.; Hupp, J. T.; Nguyen, S. T. *J. Am. Chem. Soc.* **2009**, *131*, 4204–4205.
- (75) Smithenry, D. W.; Wilson, S. R.; Suslick, K. S. *Inorg. Chem.* **2003**, *42*, 7719–7721.
- (76) Lipstman, S.; Goldberg, I. *CrystEngComm* **2010**, *12*, 52–54.
- (77) Lipstman, S.; Muniappan, S.; Goldberg, I. *Acta Crystallogr., Sect. C: Cryst. Struct. Commun.* **2007**, *63*, O371–O373.
- (78) Lipstman, S.; Muniappan, S.; George, S.; Goldberg, I. *Dalton Trans.* **2007**, 3273–3281.
- (79) George, S.; Lipstman, S.; Muniappan, S.; Goldberg, I. *Crystengcomm* **2006**, *8*, 417–424.
- (80) George, S.; Lipstman, S.; Goldberg, I. *Cryst. Growth Des.* **2006**, *6*, 2651–2654.
- (81) Barron, P. M.; Wray, C. A.; Hu, C.; Guo, Z.; Choe, W. *Inorg. Chem.* **2010**, *49*, 10217–10219.
- (82) Choi, E.-Y.; Barron, P. M.; Novotny, R. W.; Son, H.-T.; Hu, C.; Choe, W. *Inorg. Chem.* **2009**, *48*, 426–428.
- (83) Kempe, R. Z. *Anorg. Allg. Chem.* **2004**, *631*, 1038–1040.
- (84) Schareina, T.; Kempe, R. Z. *Anorg. Allg. Chem.* **2000**, *626*, 1279–1281.
- (85) Kosal, M. E.; Chou, J. H.; Wilson, S. R.; Suslick, K. S. *Nat. Mater.* **2002**, *1*, 118–121.
- (86) Kato, C. N.; Ono, M.; Hino, T.; Ohmura, T.; Mori, W. *Catal. Commun.* **2006**, *7*, 673–677.
- (87) Sato, T.; Mori, W.; Kato, C. N.; Yanaoka, E.; Kuribayashi, T.; Ohtera, R.; Shiraishi, Y. *J. Catal.* **2005**, *232*, 186–198.
- (88) Choi, E.-Y.; Wray, C. A.; Hu, C.; Choe, W. *CrystEngComm* **2009**, *11*, 553–555.
- (89) Farha, O. K.; Shultz, A. M.; Sarjeant, A. A.; Nguyen, S. T.; Hupp, J. T. *J. Am. Chem. Soc.* **2011**, *133*, 5652–5655.
- (90) Cavka, J. H.; Jakobsen, S.; Olsbye, U.; Guillou, N.; Lamberti, C.; Bordiga, S.; Lillerud, K. P. *J. Am. Chem. Soc.* **2008**, *130*, 13850–13851.
- (91) Low, J. J.; Benin, A. I.; Jakubczak, P.; Abrahamian, J. F.; Faheem, S. A.; Willis, R. R. *J. Am. Chem. Soc.* **2009**, *131*, 15834–15842.
- (92) Dan-Hardi, M.; Serre, C.; Frot, T. o.; Rozes, L.; Maurin, G.; Sanchez, C.; Férey, G. *J. Am. Chem. Soc.* **2009**, *131*, 10857–10859.
- (93) Férey, G. *Chem. Soc. Rev.* **2008**, *37*, 191–214.
- (94) Horcajada, P.; Chalati, T.; Serre, C.; Gillet, B.; Sebrie, C.; Baati, T.; Eubank, J. F.; Heurtaux, D.; Clayette, P.; Kreuz, C.; Chang, J.-S.; Hwang, Y. K.; Marsaud, V.; Bories, P.-N.; Cynober, L.; Gil, S.; Férey, G.; Couvreur, P.; Gref, R. *Nat. Mater.* **2010**, *9*, 172–178.
- (95) Fateeva, A.; Horcajada, P.; Devic, T.; Serre, C.; Marrot, J.; Grenèche, J. M.; Morcrette, M.; Tarascon, J. M.; Maurin, G.; Férey, G. *Eur. J. Inorg. Chem.* **2010**, *24*, 3789–3794.
- (96) Férey, G.; Millange, F.; Morcrette, M.; Serre, C.; Doublet, M.-L.; Grenèche, J.-M.; Tarascon, J.-M. *Angew. Chem., Int. Ed.* **2007**, *46*, 3259–3263.
- (97) Choi, S. B.; Seo, M. J.; Cho, M.; Kim, Y.; Jin, M. K.; Jung, D.-Y.; Choi, J.-S.; Ahn, W.-S.; Rowsell, J. L. C.; Kim, J. *Cryst. Growth Des.* **2007**, *7*, 2290–2293.
- (98) Horcajada, P.; Surblé, S.; Serre, C.; Hong, D.-Y.; Seo, Y.-K.; Chang, J.-S.; Grenèche, J.-M.; Margiolaki, I.; Férey, G. *Chem. Commun.* **2007**, 2820–2822.
- (99) Lupu, D.; Ardelean, O.; Blanita, G.; Borodi, G.; Lazar, M. D.; Biris, A. R.; Cloan, C.; Mihet, M.; Misan, I.; Popeneciu, G. *Int. J. Hydrogen Energy* **2011**, *36*, 3586–3592.
- (100) Yoon, J. H.; Choi, S. B.; Oh, Y. J.; Seo, M. J.; Jhon, Y. H.; Lee, T.-B.; Kim, D.; Choi, S. H.; Kim, J. *Catal. Today* **2007**, *120*, 324–329.
- (101) Devic, T.; Horcajada, P.; Serre, C.; Salles, F.; Maurin, G.; Moulin, B. a.; Heurtaux, D.; Clet, G.; Vimont, A.; Grenèche, J.-M.; Ouay, B. L.; Moreau, F.; Magnier, E.; Filinchuk, Y.; Marrot, J. m.; Lavalley, J.-C.; Daturi, M.; Férey, G. *J. Am. Chem. Soc.* **2010**, *132*, 1127–1136.
- (102) Millange, F.; Guillou, N.; Walton, R. I.; Grenèche, J.-M.; Margiolaki, I.; Férey, G. *Chem. Commun.* **2008**, 4732–4734.
- (103) Whitfield, T. R.; Wang, X.; Liu, L.; Jacobson, A. J. *Solid State Sci.* **2005**, *7*, 1096–1103.
- (104) Maurin, G.; Bell, R. G.; Devautour, S.; Giuntini, J. C.; Henn, F. *J. Phys. Chem. B* **2004**, *108*, 3739.
- (105) Maurin, G.; Llewellyn, P. L.; Kuchta, B.; Poyet, T. *J. Phys. Chem. B* **2005**, *109*, 125.
- (106) Maurin, G.; Senet, P.; Devautour, S.; Gaveau, P.; Henn, F.; Van Doren, V. E.; Giuntini, J. C. *J. Phys. Chem. B* **2001**, *105*, 9297.
- (107) Dinca, M.; Long, J. R. *J. Am. Chem. Soc.* **2007**, *129*, 11172–11176.
- (108) Mulfort, K. L.; Hupp, J. T. *J. Am. Chem. Soc.* **2007**, *129*, 9604–9605.
- (109) Nouar, F.; Eckert, J.; Eubank, J. F.; Forster, P.; Eddaoudi, M. *J. Am. Chem. Soc.* **2009**, *131*, 2864–2870.
- (110) Yang, S.; Lin, X.; Blake, A. J.; Walker, G. S.; Hubberstey, P.; Champness, N. R.; Schroder, M. *Nat. Chem.* **2009**, *1*, 487–493.
- (111) Lin, J.-B.; Xue, W.; Zhang, J.-P.; Chen, X.-M. *Chem. Commun.* **2011**, *47*, 926–928.
- (112) Procopio, E. Q.; Linares, F.; Montoro, C.; Colombo, V.; Maspero, A.; Barea, E.; Navarro, J. A. R. *Angew. Chem., Int. Ed.* **2010**, *49*, 7308–7311.
- (113) Xie, L.-H.; Lin, J.-B.; Liu, X.-M.; Wang, Y.; Zhang, W.-X.; Zhang, J.-P.; Chen, X.-M. *Inorg. Chem.* **2010**, *49*, 1158–1165.
- (114) Li, J.-R.; Kuppler, R. J.; Zhou, H. C. *Chem. Soc. Rev.* **2009**, *38*, 1477–1504.
- (115) Cheon, Y. E.; Suh, M. P. *Chem.—Eur. J.* **2008**, *14*, 3961–3967.
- (116) Dinca, M.; Yu, A. F.; Long, J. R. *J. Am. Chem. Soc.* **2006**, *128*, 8904–8913.
- (117) Humphrey, S. M.; Chang, J.-S.; Jhung, S. H.; Yoon, J. W.; Wood, P. T. *Angew. Chem., Int. Ed.* **2007**, *46*, 272–275.
- (118) Li, Y.; Yang, R. T. *Langmuir* **2007**, *23*, 12937–12944.
- (119) Ma, S.; Yuan, D.; Wang, X.-S.; Zhou, H.-C. *Inorg. Chem.* **2009**, *48*, 2072–2077.
- (120) Murray, L. J.; Dinca, M.; Yano, J.; Chavan, S.; Bordiga, S.; Brown, C. M.; Long, J. R. *J. Am. Chem. Soc.* **2010**, *132*, 7856–7857.
- (121) Tanaka, D.; Nakagawa, K.; Higuchi, M.; Horike, S.; Kubota, Y.; Kobayashi, T. C.; Takata, M.; Kitagawa, S. *Angew. Chem., Int. Ed.* **2008**, *47*, 3914–3918.
- (122) Bloch, E. D.; Murray, L. J.; Queen, W. L.; Chavan, S. M.; Maximoff, S. N.; Bigi, J. P.; Krishna, R.; Peterson, V. K.; Grandjean, F.; Long, G. J.; Smit, B.; Bordiga, S.; Brown, C. M.; Long, J. R. *J. Am. Chem. Soc.* **2011**, *133*, 14814–14822.
- (123) Zanota, M. L.; Heymans, N.; Gilles, F.; Su, B. L.; Frère, M.; De Weireld, G. *J. Chem. Eng. Data* **2010**, *55*, 448–458.
- (124) Coe, C. G.; Kirner, J. F.; Pierantozzi, R.; White, T. R. *US Patent* 1992, 5152, 813.
- (125) Fitch, F. R. *US Patent* 1995, 5464, 467.
- (126) Adler, A. D.; Longo, F. R.; Finarelli, J.; Goldmach, J.; Assour, J.; Korsakof, L. *J. Org. Chem.* **1967**, *32*, 476–477.
- (127) Farha, O. K.; Mulfort, K. L.; Thorsness, A. M.; Hupp, J. T. *J. Am. Chem. Soc.* **2008**, *130*, 8598–8599.
- (128) Xie, M.-H.; Yang, X.-L.; Wu, C.-D. *Chem. Commun.* **2011**, *47*, 5521–5523.
- (129) Sanselme, M.; Grenèche, J.-M.; Riou-Cavellec, M.; Férey, G. *Solid State Sci.* **2004**, *6* (8), 853–858.
- (130) Serre, C.; Mellot-Draznieks, C.; Surble, S.; Audebrand, N.; Filinchuk, Y.; Férey, G. *Science* **2007**, *315*, 1828–1831.
- (131) Serre, C.; Millange, F.; Thouvenot, C.; Nogues, M.; Marsolier, G.; Louer, D.; Férey, G. *J. Am. Chem. Soc.* **2002**, *124*, 13519–13526.
- (132) Düren, T.; Millange, F.; Férey, G.; Walton, K. S.; Snurr, R. Q. *J. Phys. Chem. C* **2007**, *111*, 15350–15356.
- (133) Rouquerol, J.; Llewellyn, P.; Rouquerol, F. In *Studies in Surface Science and Catalysis*; Elsevier: 2007; Vol. 160, pp 49–56.
- (134) Kosal, M. E.; Chou, J.-H.; Wilson, S. R.; Suslick, K. S. *Nat. Mater.* **2002**, *1*, 118–121.
- (135) Vanderschueren, J.; Gasiot, J. *Thermally Stimulated Relaxation in Solids*; Berlin, 1979.
- (136) Ibar, J. P. *Fundamentals of Thermally Stimulated Current and Relaxation Map Analysis*; New Canaan, 1993.

- (137) Devautour, S.; Vanderschueren, J.; Giuntini, J. C.; Henn, F.; Zanchetta, J. V.; Ginoux, J. L. *J. Phys. Chem. B* **1998**, *102*, 3749.
- (138) Kalogeras, J. M.; Vassilikou-Dova, A. *Cryst. Res. Technol.* **1996**, *31*, 693.
- (139) Nicolas, A.; Devautour-Vinot, S.; Maurin, G.; Giuntini, J. C.; Henn, F. *J. Phys. Chem. C* **2007**, *111*, 4722.
- (140) Nicolas, A.; Devautour-Vinot, S.; Maurin, G.; Giuntini, J. C.; Henn, F. *Microporous Mesoporous Mater.* **2008**, *109* (1–3), 413.
- (141) Salles, F.; Devautour-Vinot, S.; Bildstein, O.; Jullien, M.; Maurin, G.; Giuntini, J. C.; Douillard, J. M.; Van Damme, H. *J. Phys. Chem. C* **2008**, *112*, 14001.
- (142) Devautour, S.; Henn, F.; Giuntini, J. C.; V., Z. J.; Vanderschueren, J. *J. Phys. D: Appl. Phys.* **1999**, *32*, 147.
- (143) Rege, S. U.; Yang, R. T.; Buzanowski, M. A. *Chem. Eng. Sci.* **2000**, *55*, 4827–4838.
- (144) Campo, M. C.; Magalhães, F. D.; Mendes, A. *J. Membr. Sci.* **2010**, *350*, 139–147.
- (145) Chen, Y. D.; Yang, R. T.; Uawithya, P. *AIChE J.* **1994**, *40*, 577–585.
- (146) Gaffney, T. R. *Curr. Opin. Solid State Mater. Sci.* **1996**, *1*, 69–75.
- (147) Merritt, A.; Rajagopalan, R.; Foley, H. C. *Carbon* **2007**, *45* (6), 1267–1278.
- (148) Moreira, R. F. P. M.; José, H. J.; Rodrigues, A. E. *Carbon* **2001**, *39*, 2269–2276.
- (149) Reid, C. R.; O’Koy, I. P.; Thomas, K. M. *Langmuir* **1998**, *14*, 2415–2425.
- (150) Ruthven, D. M.; Raghavan, N. S.; Hassan, M. M. *Chem. Eng. Sci.* **1986**, *41*, 1325–1332.
- (151) Yoshida, S.; Ogawa, N.; Kamioka, K.; Hirano, S.; Mori, T. *Adsorption* **1999**, *5*, 57–61.
- (152) Maurin, G.; Llewellyn, P. L.; Poyet, T.; Kuchta, B. *Microporous Mesoporous Mater.* **2005**, *79* (1–3), 53–59.
- (153) Yoshida, S.; Hirano, S.; Harada, A.; Nakano, M. *Microporous Mesoporous Mater.* **2001**, *46* (2–3), 203–209.
- (154) Zanita, M.-L.; Heymans, N.; F., G.; Su, B.-L.; De Weireld, G. *Microporous Mesoporous Mater.* **2011**, *143* (2–3), 302–310.
- (155) De Weireld, G.; Frère, M.; Jadot, R. *Meas. Sci. Technol.* **1999**, *10*, 117–126.
- (156) Alt, H.; Binder, H.; Sandstede, G. *J. Catal.* **1973**, *28*, 8–19.
- (157) Tsuda, M.; Sy, Dy, E.; Kasai, H. *J. Chem. Phys.* **2005**, *122* (244719), 1–7.
- (158) Yang, J.; Huang, P. *Chem. Mater.* **2000**, *12*, 2693–2697.
- (159) Collman, J. P.; Brauman, J. I.; Doxsee, K. M.; Halbert, T. R.; Hayes, S. E.; Suslick, K. S. *J. Am. Chem. Soc.* **1978**, *100*, 2761–2766.
- (160) Trojanek, A.; Langmaier, J.; Sebera, J.; Zalis, S.; Barbe, J.-M.; Girault, H. H.; Samec, Z. *Chem. Commun.* **2011**, 5446–5448.
- (161) Nishide, H.; Tsukahara, Y.; Tsuchida, E. *J. Phys. Chem. B* **1998**, *102*, 8766–8770.
- (162) Ferraz, H. C.; Duarte, L. T.; Di Luccio, M.; Alves, T. L. M.; Habert, A. C.; Borges, C. P. *Braz. J. Chem. Eng.* **2007**, *24*, 101–118.
- (163) Yang, J. P.; Huang, P. C. *J. Appl. Polym. Sci.* **2000**, *77*, 484–488.
- (164) Xie, M.-H.; Yang, X.-L.; Zou, C.; Wu, C.-D. *Inorg. Chem.* **2011**, *50*, 5318–5320.